

Peristaltic transport of a pulsatile flow for a particle-fluid suspension through an annular region: Application of a clot blood model

Khaled S. Mekheimer^{1,*}, Mohamed S. Mohamed¹

¹Dept of Mathematics and statistics, faculty of Science, Taif University, Hawia 888, Taif, Saudi Arabia
& Dept of Mathematics, faculty of Science, Al-Azhar University, Nasr City, Cairo, EGYPT.

*Kh.Mekheimer@yahoo.com & s_math223@hotmail.com

Abstract— A serious pathological condition is encountered when some blood constituents deposited on the blood vessels get detached from the wall, join the blood stream again and form a clot. The pulsatile flow for peristaltic transport of a fluid with suspended particles may be considered as a mathematical model for the blood flow. We study this model in an annular region with a clot inside it, under low Reynolds number and long wavelength approximation. We model a small artery as a tube having a sinusoidal wave travelling down its wall with a constant velocity c and a clot model inside it. Closed form solutions are obtained for the fluid/particle velocity, as well as the stream function, and the pressure gradient. These solutions contain new additional parameters, namely, δ , the height of the clot, β , the pulsating number and C , the suspension parameter, and the wave amplitude b . The pressure rise and friction force on the outer tube have been discussed for various values of the physical parameters of interest. Finally, the trapping phenomenon is illustrated.

Index Terms— pulsatile flow; peristaltic pumping; Annulus flow; Clot blood model

1 INTRODUCTION

Peristaltic pumping is a form of fluid transport that occurs when a progressive wave of area contraction or expansion propagates along the length of a distensible duct. Peristalsis is an inherent property of many biological systems having smooth muscle tubes that transports biofluids by its propulsive movement and is found in the transport of urine from kidney to the bladder, the movement of chyme in the gastrointestinal tract, intra-uterine fluid motion, vasomotion of the small blood vessels and in many other glandular ducts. The mechanism of peristaltic transport has been exploited for industrial applications such as sanitary fluid transport, blood pumps in heart-lung machine and transport of corrosive fluids where the contact of the fluid with the machinery parts is prohibited [1-12].

Blood being a suspension of corpuscles, at low shear rates behaves like a non-Newtonian fluid in small arteries. Besides, the theoretical analysis of Haynes [13] and experimental observations of Cokelet [14] indicate that blood can not be treated as a single-phase homogeneous viscous fluid in narrow arteries (of diameter ≤ 1000 μm). The individuality of red cells (of diameter 8 μm) is important even in such large vessels with diameter up to 100 cells' diameter. Moreover, an accurate description of flow requires consideration of red cells as discrete particles. It is to note that the average hematocrit in human blood under normal health conditions lies between 40-45 percent. In addition, certain observed phenomena in blood including the Fahraeus-Lindqvist effect, non-Newtonian behaviour, etc. can not be explained fully by treating blood as a single-phase fluid. The individuality of erythrocytes can not therefore be ignored while dealing with the prob-

lem of microcirculation also. It seems to be therefore necessary to treat the whole blood as a particle-fluid (erythrocyte-plasma) system while flowing through narrow arteries.

The interaction of purely periodic mean flow with a peristaltic induced flow is investigated within the framework of a two-dimensional analogue has been studied by N.A.S.Afifi and N.S.Gad [15]. Eytan and Elad [16] have developed a mathematical modal of wall-induced peristaltic fluid flow in two-dimensional channel with wave trains having a phase difference moving independently on the upper and lower walls to simulate intra-uterine fluid motion in a sagittal cross-section of the uterus. They have used the lubrication theory to obtain a time dependent flow solution in a fixed frame. The results obtained by Eytan and Elad [16] have been used to evaluate the fluid flow pattern in a non-pregnant uterus.

The rheological studies of steady flow of blood are useful in providing reference information on the rheological characteristics of blood, for clinical purpose, in viscometers. On the other hand, in reality, blood flow in arterial system is pulsatile, with time varying characteristics, which even extends into the capillarity bed. Ariman et al. [17] have studied pulsatile flow of blood assuming different modals, they have studied the steady and pulsatile flow of micropolar fluid and have obtained the exact solution for velocity and cell rotation velocity in the form of Bessel-Fourier series.

With the above discussion, we are interested to investigate the effect of the pulsatile flow on peristaltic motion of an incompressible particle-fluid suspension through a region with flexible walls and a clot inside it.

2. Formulation and analysis of the physical problem

Consider peristaltic transport of an incompressible Newtonian fluid in the region between two coaxial cylinders [18].

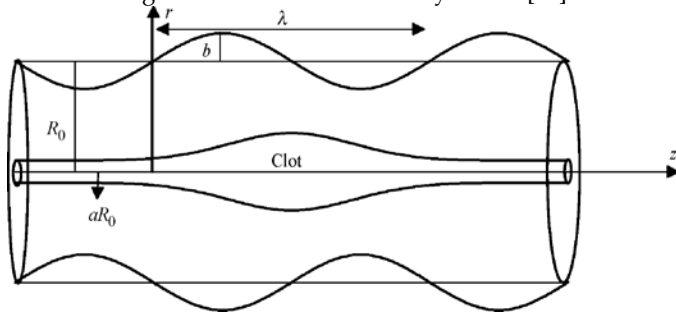


Figure 1. Problem geometry .

The geometries of the cylinders wall surfaces are (see Figure 1).

$$R' = R'_0(a_0 + f(Z', t')), \quad 0 \leq Z' \leq \lambda \quad (1)$$

$$= R_0 a_0 \quad \text{otherwise}$$

$$h = R'_0 + b \sin\left(\frac{2\pi}{\lambda}(Z' - ct')\right), \quad (2)$$

$a_0 R_0$ is the radius of the inner cylinder and this keeps the clot model in position inside the cylinder with $a_0 \ll 1$, $f(Z', t')$ represent an arbitrary shape along the axial direction, R_0 is the radius of the outer cylinder at any axial distance Z' from the inlet, the wavelength and the wave amplitude are λ and b respectively, the propagation velocity of the wave is c and t' is the time. A wave frame (r', z') is introduced and moving with velocity c away from the fixed frame (R', Z') .

The governing equations for the flow problem, with no external forces, are given by[7],

For a fluid Phase:

$$\frac{\partial}{\partial Z'}(1-C)U'_f + \frac{\partial}{\partial R'}(1-C)W'_f + \frac{(1-C)W'_f}{R'} = 0 \quad (3)$$

$$(1-C)\rho_f \left[\frac{\partial U'_f}{\partial t'} + U'_f \frac{\partial U'_f}{\partial Z'} + W'_f \frac{\partial U'_f}{\partial R'} \right] = -(1-C) \frac{\partial p'}{\partial Z'} +$$

$$(1-C)\mu_s(C) \left[\frac{\partial^2 U'_f}{\partial Z'^2} + \frac{\partial^2 U'_f}{\partial R'^2} + \frac{1}{R'} \frac{\partial U'_f}{\partial R'} \right] + C s (U'_p - U'_f) \quad (4)$$

$$(1-C)\rho_f \left[\frac{\partial W'_f}{\partial t'} + U'_f \frac{\partial W'_f}{\partial Z'} + W'_f \frac{\partial W'_f}{\partial R'} - \frac{W'^2_f}{R'} \right] =$$

$$-(1-C) \frac{\partial p'}{\partial R'} + (1-C)\mu_s(C) \left[\frac{\partial^2 W'_f}{\partial Z'^2} + \frac{\partial^2 W'_f}{\partial R'^2} + \frac{1}{R'} \frac{\partial W'_f}{\partial R'} - \frac{W'^2_f}{R'^2} \right] +$$

$$C s (W'_p - W'_f) \quad (5)$$

For a particle phase''

$$\frac{\partial}{\partial Z'} C U'_p + \frac{\partial}{\partial R'} C W'_p + \frac{C W'_p}{R'} = 0 \quad (6)$$

$$C \rho_p \left[\frac{\partial U'_p}{\partial t'} + U'_p \frac{\partial U'_p}{\partial Z'} + W'_p \frac{\partial U'_p}{\partial R'} \right] = -C \frac{\partial p'}{\partial Z'} + C s (U'_f - U'_p) \quad (7)$$

$$C \rho_p \left[\frac{\partial W'_p}{\partial t'} + U'_p \frac{\partial W'_p}{\partial Z'} + W'_p \frac{\partial W'_p}{\partial R'} - \frac{W'^2_p}{R'} \right] = -C \frac{\partial p'}{\partial R'} + C s (W'_f - W'_p) \quad (8)$$

where (W'_f, U'_f) and (W'_p, U'_p) are the velocity components of the fluid and the particle phase in R and Z -directions, respectively, P' is the pressure, C is the constant (Srivastava and Saxena, volume fraction density of the particles, $\mu_s(C)$ is the mixture viscosity (effective or apparent viscosity of suspension) and S is the drag coefficient of interaction for the force exerted by one phase on the other. The expression for the drag coefficient of interaction, S and the empirical relation for the viscosity of the suspension, μ_s for the present problem is selected as [7],

$$S = \frac{9}{2} \frac{\mu_0}{a_0^2} \lambda'(C),$$

$$4Cm\lambda'(C) = \frac{4 + [8C - 3C^2]^{1/2} + 3C}{(2 - 3C)^2},$$

$$4Cm\mu_s = \mu_s(C) = \frac{\mu_0}{1 - mC},$$

$$m = 0.070 \exp \left[2.49C + \frac{1107}{T} \exp(-1.69C) \right],$$

where a^*_0 is the radius of each solid particle suspended in the fluid, μ_0 is the constant fluid viscosity and T is measured in absolute temperature ($^{\circ}\text{K}$). The formula has been tested by Charm and Kurland [19] by using a cone and a plate viscometer, and it has been proclaimed that it is reasonably accurate up to $C = 0.6$. The related equation between the laboratory and the wave frame are:

$$z' = Z' - ct' ; \quad r' = R' \quad (9)$$

and the velocity components for the fluid and particle are also related by

$$u'_{f,p}(r', z') = U'_{f,p}(R', Z' - ct') ;$$

$$w'(r', z') = W'(R', Z' - ct') - c \quad (10)$$

u' and w' are defined as the velocity components in the wave frame. Using the following dimensionless variables

$$\begin{aligned} p &= \frac{R_0^2}{\mu c \lambda} p', \quad w_{f,p} = \frac{\lambda w'_{f,p}}{R_0 c}, \quad u_{f,p} = \frac{u'_{f,p}}{c} t = \frac{1}{T_0} t' \\ , Re &= \frac{\rho_f c R_0}{\mu_s (1-C)}, \quad \rho' = \frac{\rho_p}{\rho_f}, \quad r = \frac{1}{R_0} r' \\ , \phi &= \frac{b}{R_0}, \quad \delta^* = \frac{R_0}{\lambda}, \quad z = \frac{z'}{\lambda} \quad (11) \\ \bar{\mu} &= \frac{\mu_s}{\mu_0}, \quad M = \frac{s R_0^2}{(1-C) \mu_s}, \quad r_1 = \frac{r'_1}{R_0} = \varepsilon, \\ r_2 &= \frac{r'_2}{R_0} = 1 + \phi \cos(2\pi z), \end{aligned}$$

where μ_0 is the viscosity coefficient and T_0 represent the characteristic time of the flow. After defining the dimensionless stream function by [7].

$$u_{f,p}(r, z) = -\frac{1}{r} \frac{\partial \psi_{f,p}}{\partial r} ; \quad w_{f,p}(r, z) = \frac{1}{r} \frac{\partial \psi_{f,p}}{\partial z} \quad (12)$$

the continuity equation is satisfied, and the equations of motion take the form

For fluid phase:

$$\begin{aligned} (1-C) \left[-\delta^{*2} \beta \frac{\partial}{\partial t} + R_e \delta^{*3} \left(\frac{1}{r} \frac{\partial \psi_f}{\partial z} \frac{\partial}{\partial r} - \frac{1}{r} \frac{\partial \psi_f}{\partial r} \frac{\partial}{\partial z} \right) \right] \frac{1}{r} \frac{\partial \psi_f}{\partial z} \\ = -(1-c) \frac{\partial p}{\partial r} + (1-C) \mu \left(-\delta^{*2} \frac{1}{r} \frac{\partial}{\partial r} \left(r \frac{\partial}{\partial r} \left(\frac{1}{r} \frac{\partial \psi_f}{\partial z} \right) \right) \right) \\ \left(-\delta^{*4} \frac{\partial}{\partial z} \left(\frac{\partial}{\partial z} \left(\frac{1}{r} \frac{\partial \psi_f}{\partial z} \right) \right) \right) \\ + \delta^{*2} \frac{Cs}{r} \left(\frac{\partial \psi_p}{\partial z} - \frac{\partial \psi_f}{\partial z} \right) \end{aligned} \quad (13)$$

$$\begin{aligned} (1-C) \left[\beta \frac{\partial}{\partial t} + R_e \delta^{*3} \left(\frac{1}{r} \frac{\partial \psi_f}{\partial z} \frac{\partial}{\partial r} - \frac{1}{r} \frac{\partial \psi_f}{\partial r} \frac{\partial}{\partial z} \right) \right] \frac{1}{r} \frac{\partial \psi_f}{\partial r} \\ - (1-C) \frac{\partial p}{\partial z} \\ + (1-C) \mu \left(\frac{1}{r} \frac{\partial}{\partial r} \left(r \frac{\partial}{\partial r} \left(\frac{1}{r} \frac{\partial \psi_f}{\partial r} \right) \right) + \delta^{*2} \frac{\partial}{\partial z} \left(\frac{\partial}{\partial z} \left(\frac{1}{r} \frac{\partial \psi_f}{\partial r} \right) \right) \right) \\ - \frac{Cs}{r} \left(\frac{\partial \psi_p}{\partial r} - \frac{\partial \psi_f}{\partial r} \right) \end{aligned} \quad (14)$$

For Particle phase:

$$\begin{aligned} C \left[-\delta^{*2} \beta \frac{\partial}{\partial t} + R_e \delta^{*3} \left(\frac{1}{r} \frac{\partial \psi_p}{\partial z} \frac{\partial}{\partial r} - \frac{1}{r} \frac{\partial \psi_p}{\partial r} \frac{\partial}{\partial z} \right) \right] \frac{1}{r} \frac{\partial \psi_p}{\partial z} \\ - C \frac{\partial p}{\partial r} + \delta^{*2} \frac{Cs}{r} \left(\frac{\partial \psi_f}{\partial z} - \frac{\partial \psi_p}{\partial z} \right) \end{aligned} \quad (15)$$

$$\begin{aligned} C \left[\beta \frac{\partial}{\partial t} + R_e \delta^{*3} \left(\frac{1}{r} \frac{\partial \psi_p}{\partial z} \frac{\partial}{\partial r} - \frac{1}{r} \frac{\partial \psi_p}{\partial r} \frac{\partial}{\partial z} \right) \right] \frac{1}{r} \frac{\partial \psi_p}{\partial r} \\ - \frac{Cs}{r} \left(\frac{\partial \psi_f}{\partial r} - \frac{\partial \psi_p}{\partial r} \right) = -C \frac{\partial p}{\partial z} \end{aligned} \quad (16)$$

The dimensionless wave number δ^* , and the Womersley number

$$\beta \text{ are defined by [2] } \quad \delta^* = \frac{R_0}{\lambda}, \quad \beta = \frac{\rho R_0^2}{\mu T_0}$$

Equations given by (13-16) coincide with those in [?] for

$\beta = 0$ and $C=0$ (flow in the wave frame). Let the peristaltic flow is superposed by an oscillating flow, in this frame. So, the flow

is unsteady in the wave frame. Following the analysis given by [7] we can get,

$$\theta(t) = F(t) + 1 + \frac{\phi^2}{2} - \varepsilon^2 \quad (17)$$

With

$$\theta(t) = \frac{\bar{Q}(\bar{t})}{2\pi c R_0^2} \quad \text{and} \quad F(t) = \frac{\bar{q}(\bar{t})}{2\pi c R_0^2} \quad (18)$$

Here, $\theta(t)$ and $F(t)$ are the flow rates in the fixed and the wave frame respectively. The boundary conditions for this wave frame are [2]

$$\psi_f = 0, \quad \left(\frac{1}{r} \frac{\partial \psi_f}{\partial r} \right) = -1 \quad \text{for} \quad r = a \quad (19)$$

$$\psi_f = F(t), \quad \left(\frac{1}{r} \frac{\partial \psi_f}{\partial r} \right) = -1 \quad \text{for} \quad r = h \quad (20)$$

Also, $\mathbf{h}(z) = 1 + \phi \sin(2\pi z)$, $\mathbf{a} = \mathbf{a}(z)$ represents the dimensionless radii of the outer and inner tubes respectively.

It is impossible to solve the system equations (13-16) for arbitrary values of all parameters. The assumptions that one or more of these parameters are zero or small are widely used by many authors [2,15,16]. We carry out these assumptions in our analysis, $\delta^* \ll 1$ and $\text{Re} \ll 1$, the system (13-16) becomes

$$\frac{\partial p}{\partial r} = 0$$

$$\begin{aligned} (1-C)\beta \frac{\partial}{\partial t} \left(\frac{1}{r} \frac{\partial \psi_f}{\partial r} \right) &= -(1-C) \frac{\partial p}{\partial z} + \\ (1-C)\mu \frac{1}{r} \frac{\partial}{\partial r} \left(r \frac{\partial}{\partial r} \left(\frac{1}{r} \frac{\partial \psi_f}{\partial r} \right) \right) &+ \frac{Cs}{r} \left(\frac{\partial \psi_p}{\partial r} - \frac{\partial \psi_f}{\partial r} \right) \quad (21) \\ C\beta \frac{\partial}{\partial t} \left(\frac{1}{r} \frac{\partial \psi_p}{\partial r} \right) &= -C \frac{\partial p}{\partial z} + \frac{Cs}{r} \left(\frac{\partial \psi_f}{\partial r} - \frac{\partial \psi_p}{\partial r} \right) \end{aligned}$$

The boundary conditions are the same as in (19) and (20).

4. Perturbation solution development

Suppose that the flow rate $F(t)$ in the wave frame resulting of this interaction is given by.

$$F(t) = F_0 + \beta F_1(t) \quad (22)$$

Where, F_0 is the flow rate in the wave frame in absence of the pulsatile flow, $\bar{F}(\bar{t})$ the dimensional flow rate in the wave frame. We seek solution in the form[2]:

$$\psi_{f,p} = \psi_{0f,p} + \beta \psi_{1f,p} + \beta^2 \psi_{2f,p} \quad (23)$$

$$p = p_0 + \beta p_1 + \beta^2 p_2 \quad (24)$$

substituting (23), (24) into (19-21) and collecting terms of equal powers of β , we obtain the following set of equations.

Zeroth-order system:

$$\begin{aligned} \frac{\partial p_0}{\partial r} &= 0 \\ (1-C) \frac{\partial p_0}{\partial z} &= \\ (1-C)\mu \frac{-1}{r} \frac{\partial}{\partial r} \left(r \frac{\partial}{\partial r} \left(\frac{1}{r} \frac{\partial \psi_{0f}}{\partial r} \right) \right) &+ \frac{Cs}{r} \left(\frac{\partial \psi_{0p}}{\partial r} - \frac{\partial \psi_{0f}}{\partial r} \right) \quad (25) \end{aligned}$$

$$C \frac{\partial p_0}{\partial z} = \frac{Cs}{r} \left(\frac{\partial \psi_{0f}}{\partial r} - \frac{\partial \psi_{0p}}{\partial r} \right)$$

$$\psi_{0f} = 0, \quad \frac{1}{r} \frac{\partial \psi_{0f}}{\partial r} = -1 \quad \text{for} \quad r = a(z)$$

$$\psi_{0f} = F_0, \quad \frac{1}{r} \frac{\partial \psi_{0f}}{\partial r} = -1 \quad \text{for} \quad r = h(z)$$

First-order system:

$$\begin{aligned} \frac{\partial p_1}{\partial r} &= 0 \\ (1-C) \frac{\partial p_1}{\partial z} &= \\ (1-C)\mu \frac{-1}{r} \frac{\partial}{\partial r} \left(r \frac{\partial}{\partial r} \left(\frac{1}{r} \frac{\partial \psi_{1f}}{\partial r} \right) \right) &+ \frac{Cs}{r} \left(\frac{\partial \psi_{1p}}{\partial r} - \frac{\partial \psi_{1f}}{\partial r} \right) \quad (26) \end{aligned}$$

$$C \frac{\partial p_1}{\partial z} = \frac{Cs}{r} \left(\frac{\partial \psi_{1f}}{\partial r} - \frac{\partial \psi_{1p}}{\partial r} \right)$$

$$\psi_{1f} = 0, \quad \frac{1}{r} \frac{\partial \psi_{1f}}{\partial r} = 0 \quad \text{for} \quad r = a(z)$$

$$\psi_{1f} = F_1(t) \quad , \quad \frac{1}{r} \frac{\partial \psi_{1f}}{\partial r} = 0 \quad \text{for} \quad r = h(z) \quad u_1(r, z, t) = (\bar{\mu}(1-C)) \left(\frac{16 F_1(t)}{B^*(a^2 - h^2)} \right) \times$$

Zeroth-order solution:

$$\psi_0(r, z, t) = \frac{(\bar{\mu}(1-C))8}{B^*} \left(\frac{2 F_0(t)}{(a^2 - h^2)} - 1 \right) \times$$

$$\left[\frac{r^4 - a^4}{16} + \frac{(a^2 - h^2)}{4 \log \left[\frac{a}{h} \right]} \left(\frac{r^2 \log \left[\frac{a}{r} \right]}{2} - \frac{(a^2 - r^2)}{4} \right) + \frac{a^2(a^2 - r^2)}{8} \right] + \frac{(a^2 - r^2)}{2}$$

$$u_0(r, z, t) = \frac{(\bar{\mu}(1-C))8}{B^*} \left(\frac{2 F_0(t)}{(a^2 - h^2)} - 1 \right) \times$$

$$\left[\frac{r^2 - a^2}{4} + \frac{(a^2 - h^2) \log \left[\frac{a}{r} \right]}{4 \log \left[\frac{a}{h} \right]} \right] - 1$$

$$\frac{\partial p_0}{\partial z} = \bar{\mu}(1-C) \frac{8}{B^*} \left(\frac{2 F_0}{a^2 - h^2} - 1 \right)$$

First-order solution:

$$\psi_1(r, z, t) = \frac{\bar{\mu}(1-C)16 F_1(t)}{B^*(a^2 - h^2)} \times$$

$$\left[\frac{r^4 - a^4}{16} + \frac{(a^2 - h^2)}{4 \log \left[\frac{a}{h} \right]} \left(\frac{r^2 \log \left[\frac{a}{r} \right]}{2} - \frac{(a^2 - r^2)}{4} \right) + \frac{a^2(a^2 - r^2)}{8} \right]$$

$$\left[\frac{r^2 - a^2}{4} + \frac{(a^2 - h^2) \log \left[\frac{a}{r} \right]}{4 \log \left[\frac{a}{h} \right]} \right]$$

$$\frac{\partial p_1}{\partial z} = \frac{\bar{\mu}(1-C)16 F_1(t)}{B^*(a^2 - h^2)}$$

$$B^* = -(a^2 + h^2) + 2h^2 + 2(a^2 - \frac{a^2 - h^2}{2 \log \left[\frac{a}{h} \right]})$$

By summing up, the perturbation solution for the stream function will take the form :

$$\psi(r, z, t) = \left(\frac{\bar{\mu}(1-C)16 F(t)}{B^*(a^2 - h^2)} - \frac{8}{B^*} \right) \times$$

$$\left[\frac{r^4 - a^4}{16} + \frac{(a^2 - h^2)}{4 \log \left[\frac{a}{h} \right]} \left(\frac{r^2 \log \left[\frac{a}{r} \right]}{2} - \frac{(a^2 - r^2)}{4} \right) + \frac{a^2(a^2 - r^2)}{8} \right]$$

$$u(r, z, t) = \left(\frac{\bar{\mu}(1-C)16 F(t)}{B^*(a^2 - h^2)} - \frac{8}{B^*} \right) \times$$

$$\left[\frac{r^2 - a^2}{4} + \frac{(a^2 - h^2) \log \left[\frac{a}{r} \right]}{4 \log \left[\frac{a}{h} \right]} \right] - 1$$

$$\frac{\partial p}{\partial z} = \frac{(\bar{\mu}(1-C)16 F(t))}{B^*(a^2 - h^2)} - \frac{8}{B^*}$$

The pressure rise Δp and the friction force F_λ^0 on the outer wall with length λ in their non-dimensional forms are given by

$$\Delta p(t) = \int_0^1 \frac{\partial p}{\partial z} dz \quad \& \quad F_{\lambda}^{\circ}(t) = \int_0^1 h^2 \left(-\frac{\partial p}{\partial z} \right) dz$$

5. Results and discussions

For this work, we are interested to illustrate the effects due to the pulsatile flow

For a fluid with suspended particles in the region between two concentric cylinders, the inner one has a clot on it. the flow rate formula is given by

$$\theta(t) = \theta_0 + \beta \sin(2\pi t).$$

This section is divided into two subsections. In the first subsection, The effects of various parameters on the pulsating pumping interaction characteristics of the fluid through an annulus region are investigated. The trapping phenomena of the pulsating flow with peristalsis is illustrated in the second subsection. The surface geometry of the clot is [10],

$a(z) = a_0 + \delta e^{-\pi^2(z-zd-0.5)^2}$ where δ is the maximum height attained by the clot at $z = zd + 0.5$, a_0 is radius ratio of the inner tube that keeps the clot in position and zd represents the axial displacement of the clot[10].

5.1 Pulsating-Pumping interaction characteristics

The influences of various emerging parameters of our analysis on the pressure rise per wavelength Δp and the friction force F_{λ}° , on the wall cylinder is described in this subsection. The effect of these parameters are shown in figures (2-7). These figures describes the variation of Δp , and F_{λ}° , with $\theta(t)$ for various values of β , δ , C and zd .

First, in the absence of the pulsatile flow the distribution of Δp , and F_{λ}° , versus the dimensionless flow rate θ are illustrated in figures (2a,b), we see from these figures that the relation between Δp and θ are linear and coincide with those found by several authors[1-3,10,11]. The graph in figure (2a) is sectorized so that quadrant I is the peristaltic pumping, quadrant II is the augmented flow, quadrant IV is called retrograde or backward pumping and there is no flows in quadrant III [10]. The case where the peristaltic transport is superposed to oscillating flow(

$\beta \neq 0$) and for every positive median value of θ_0 , abscissa of one point of a straight line D of the figure (2a) for which $\Delta p, > 0$, we observe that the distributions of Δp , and F_{λ}° , versus the flow rate θ become ellipsis whose the principal and the median shafts increase with increasing β [2], figure (3a&b). Changes occurs in the principal shaft direction with increasing the model from the tube to a clot model figure(3b). This change in the principal shaft direction is obvious as for changing the model geometry, as δ increases, while slightly changes for the shift displacement of the clot figure(4 &5). Also from these figures, the pressure rise values increases as δ increases. Figure(6) show the variation of Δp with C Figure (7) shows the variation of the dimensionless friction force on the outer wall cylinder, and indicate that the friction forces have the opposite behaviour compared to pressure rise [10].

5.2 Stream lines and trapping phenomena

A volume of fluid bounded by a closed stream line in the wave frame is defied as a "bolus" transported at the wave speed, and such phenomena called a trapping phenomenon[2].

Figures (8-12) illustrates the streamline graphs for different values of the clot height δ , the pulsating parameter β , the shift displacement of the clot, the wave amplitude ϕ and the flow rate θ . It is observed that as the clot height increase the symmetry of the stream lines is broken and the flow is shifted upper towards the outer cylinder and the flow moves through a narrow region between the two cylinders. The bolus of the trapping is obvious whence the oscillating flow appears and the size of the trapping bolus increase as β increase. Figure (11) illustrate the effect of the shift displacement on the stream lines. For small wave amplitude, smooth stream lines are appears, but ϕ as increases a sinusoidal pattern for the stream lines is expected according to the sinusoidal waves generated on the outer wall cylinder. Finally, the effect of the wave amplitude ϕ and the flow rate are illustrated in figure(11&12), which shows the appearance of the bolus trapped in the region closed the outer wall cylinder.

6. Conclusion

- The pressure rise and flow rate relation is a linear one for a steady frame of reference and this relation become a non-linear for the unsteady case (pulsating flow).
- The pressure rise is higher for an annulus with a clot than that for a tube.
- For a suspended particles with a fluid the pressure rise bcome smaller as C increases.
- The shift displacement clot occurs a sleight effect on the pressure rise.
- The stream lines moves towards the outer wall cylinder as the clot height increase
- The trapping phenomena is obvious for the pulsatin flow than that for the steady one.
- Trapping bolus appeared in the peak wave of the stream lines as the flow rate increases.

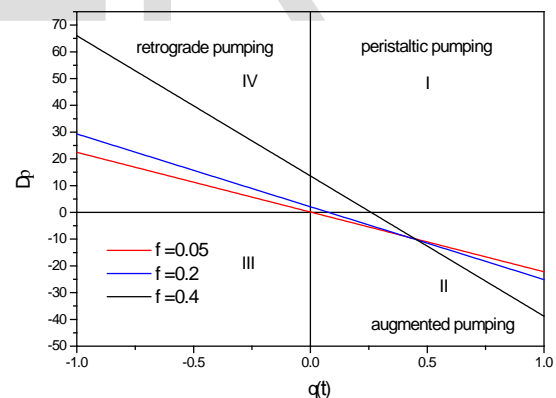
ACKNOWLEDGEMENT

THIS PAPER WAS FUNDED BY THE DEANSHIP OF SCIENTIFIC RESAEARCH (DSR), TAIF UNIVERSITY(TU) UNDER THE GRANT NUMBER (1-435-3068).THE AUTHORS ACKNOWLEDGETECHNICAL AND FINANCIAL SUPPORT OF TAIF UNIVERSITY. THE SUPPORT IS IN THE FORM OF A PROJECT FOR ACADEMIC RESEARCH AT TU.

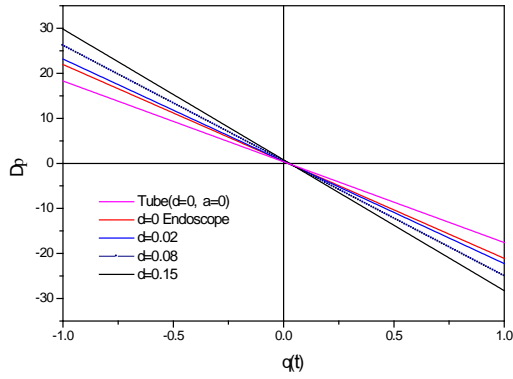
REFERENCES

- [1] K. K. Raju and R. Devanathan, "Peristaltic motion of a non-Newtonian fluid," *Rheologica* .no. 2, pp. 170–178, 1972. *Acta*, vol. 11
- [2] G. B' ohme and R. Friedrich, "Peristaltic flow of viscoelastic liquids," *Journal of Fluid Mechanics*, vol ,128.pp. 109–122, 1983.
- [3] L. M. Srivastava and V. P. Srivastava, "Peristaltic transport of blood: Casson model—II," *Journal of Biomechanics*, vol. 17, no. 11, pp. 821–829, 198
- [4]Kh. S. Mekheimer, "Peristaltic transport of a couple stress fluid in a uniform and non- uniformchannels," *Biorheology*, vol. 39, no. 6, pp. 755–765, 2002.
- [5] N. Ali, T. Hayat, and M. Sajid, "Peristaltic flow of a couple stress fluid in an asymmetric channel,"*Biorheology*, vol. 44, no. 2, pp. 125–138, 2007.
- [6] Kh. S. Mekheimer and Y. Abd Elmaboud, "Peristaltic flow of a couple stress fluid in an annulus: application of an endoscope," *Physica A*, vol. 387, no. 11, pp. 2403–2415, 2008.
- [7] V.P. Srivastava and Rashmi Srivastava , *Particulate suspension blood flow through a narrow catheterized artery*, *Computers and Mathematics with Applications* 58 (2009) 227_238
- [8] D. Philip and P. Chandra, "Peristaltic transport of simple microfluid," *Proceedings of the National Academy of Sciences, India. Section A*, vol. 65, no. 1, pp. 63–74, 1995.
- [9] P. Muthu, B. V. Rathish Kumar, and P. Chandra, "On the influence of wall properties in the peristaltic motion of micropolar fluid," *The ANZIAM Journal*, vol. 45, no. 2, pp. 245–260, 2003.

- [10] Kh. S. Mekheimer and M. A. El Kot , *SUSPENSION MODEL FOR BLOOD FLOWTHROUGH ARTERIAL CATHETERIZATION*, *Chem. Eng. Comm.*, 197:1195–1214, 2010
- [11] Kh. S. Mekheimer, Elsayed F. El Shehawey and A. M. Elaw, *Peristaltic Motion of a Particle fluid Suspension in a Planar Channel*, *International Journal of Theoretical Physics*, Vol. 37, No. 11, 1998.
- [12]R. GirijaDevi and R. Devanathan, "Peristaltic transport of micropolar fluid," *Proceedings of The National Academy of Sciences, India. Section A*, vol. 81, pp. 149–163, 1975.
- [13] R.H. Haynes, *Physical basis on dependence of blood viscosity on tube radius*, *Am. J. Physiol.* 198 (1960) 1193_1205.
- [14] G.R. Cokelet, et al., in: Y.C. Fung (Ed.), *The Rheology of Human Blood: In Biomechanics*, Prentice Hall, Englewood Cliffs, NJ, 1972.
- [15] N.A.S. Afifi and N.S.Gad , *Interaction of peristaltic flow with pulsatile fluid through a Porous medium*, *Applied Mathematics and Computation*, 142 (2003)167-176.
- [16] O Eytan and D Elad, *Analysis of intra-uterine fluid motion induced by uterine contractions*, *Bull.Math.Biol.* 61 (1999) 221
- [17] Ariman, T., Turk, M.A and Sylvester, N.D, *Steady and pulsatile blood flow*, *J.Appl.Mech (ASME)*, 41 (1974) 1-7.
- [18] Kh. S Mekheimer., and Y. Abd elmaboud, *The influences of a micropolar fluid on peristaltic transport in an annulus: Application of a clot model*, *J. Applied Bionic and Biomech.*, vol.5, No 1, 13-23, 2008.
- [19] Charm SE, Kurland GS. 1974. *Blood flow and microcirculation*. New York: John Wiley.



(a)



(b)

Figure 2 Pressure rise ΔP vs. flow rate (a) for different values ϕ and (b) for different values of δ for $\beta = 0, C=0.1$

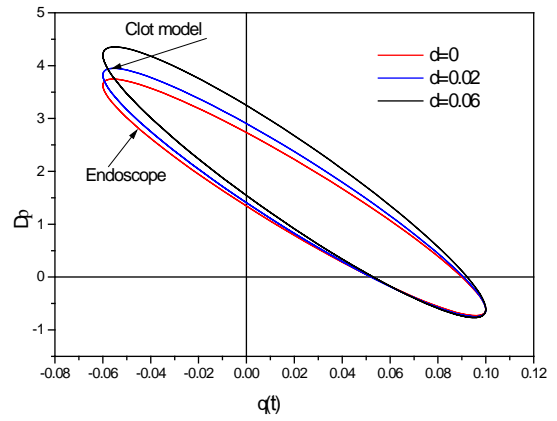
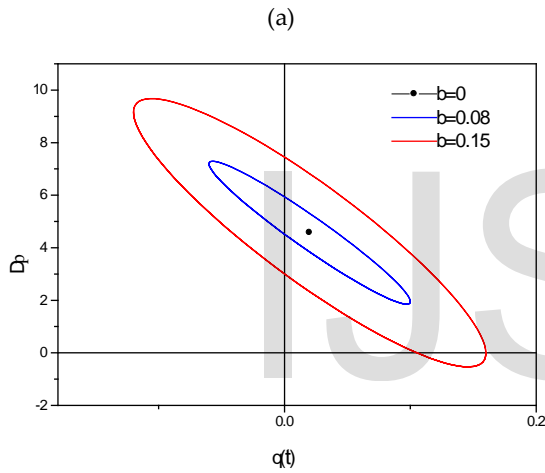


Figure 4 Pressure rise ΔP vs. flow rate for different values $\delta, \phi=0.15, z_d=0.04, C=0.1$



(a)

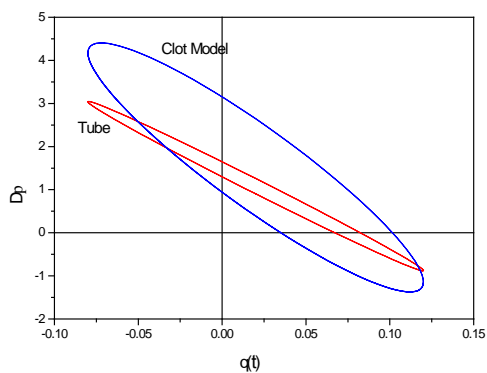


Figure 3 Pressure rise ΔP vs. flow rate (a) for different values β and (b) for tube and clot model $\phi=0.2, C=0.1$

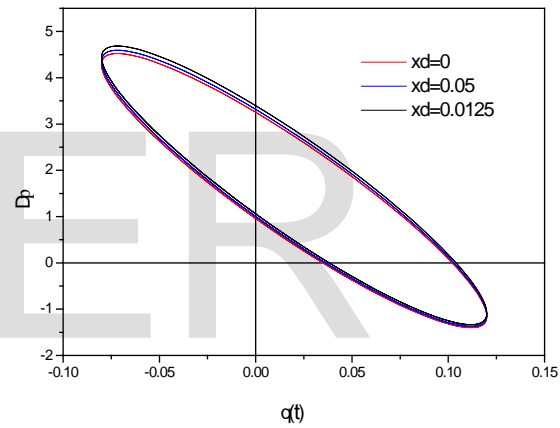


Figure 5 Pressure rise ΔP vs. flow rate for different values $z_d, \phi=0.2$ and $\delta=0.1$ for $\beta = 0.05, C=0.1$

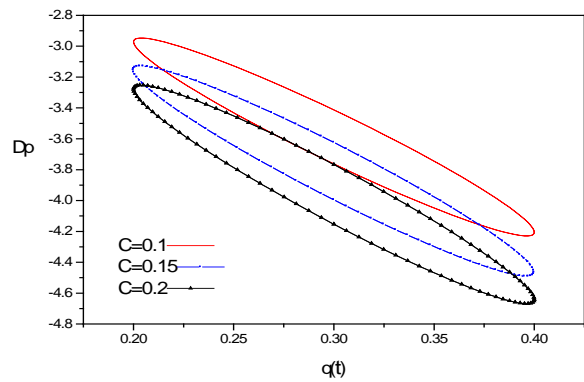


Figure 6 Pressure rise ΔP vs. flow rate for different values $C, z_d=0.1, \phi=0.2$ and $\delta=0.1$ for $\beta = 0.05$

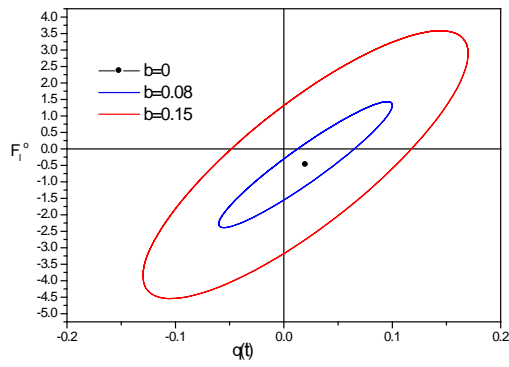


Figure 7 frictional force vs flow rate for different values $\beta, \phi=0.2$ and $\delta=0.1$ for $C=0.1, z_d=0.05$

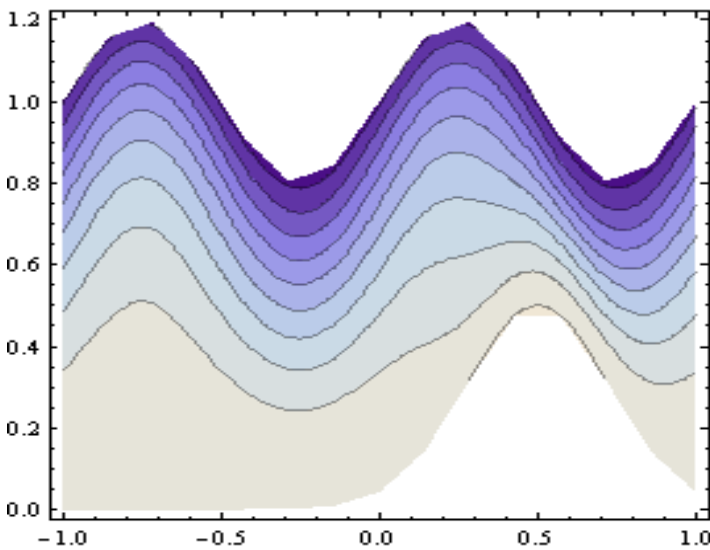
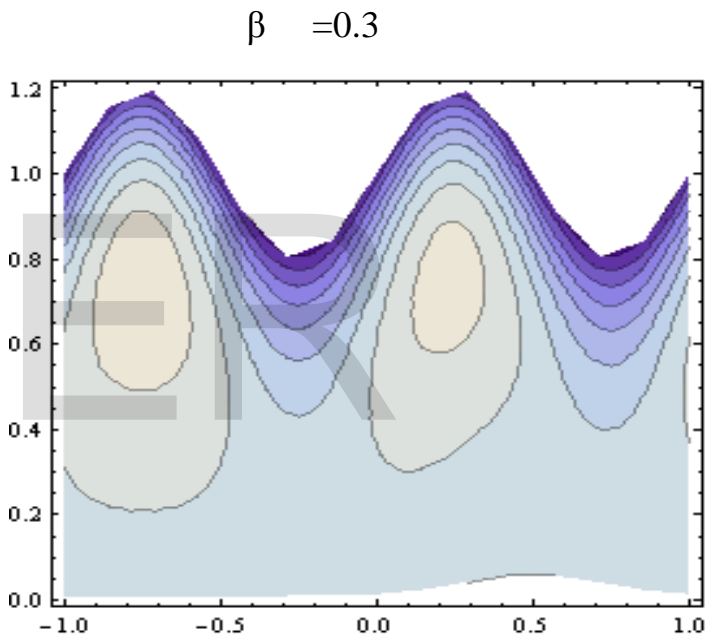
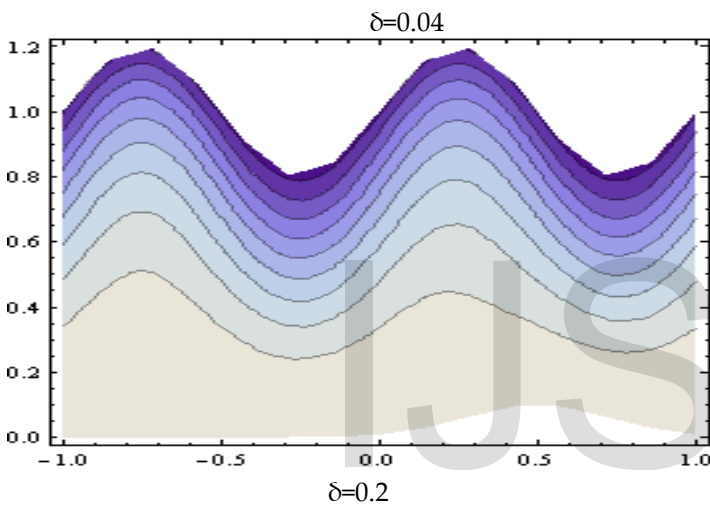
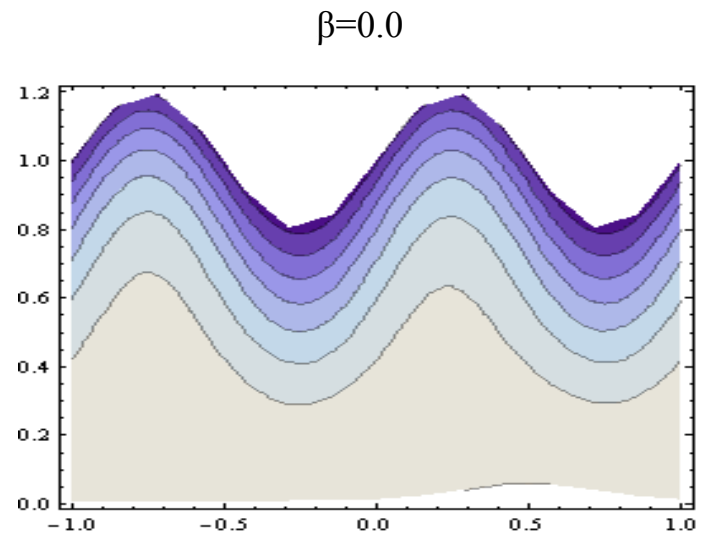
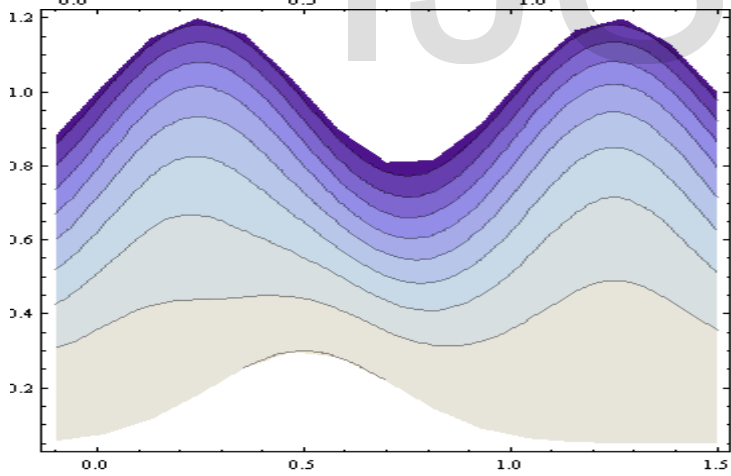
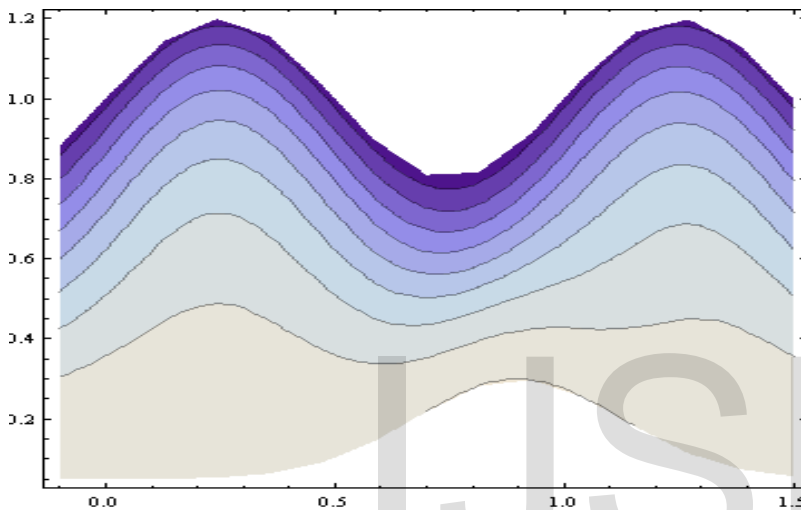


Figure 9 Contour stream lines for different values $\beta, \phi=0.2, \delta=0.1, \theta_0=0.4$ and $z_d=0.05, C=0.1$

Figure 8 Contour stream lines for different values $\delta, \phi=0.2, \beta=0.1, \theta_0=0.4$, for $z_d=0.05, C=0.1$

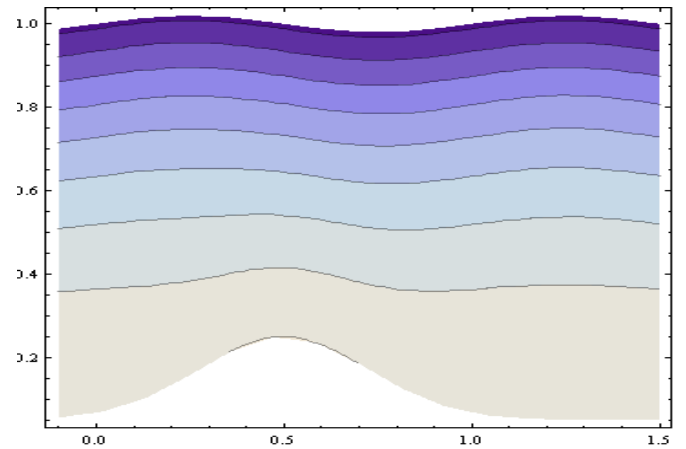
$z_d=0.0$



$z_d=0.5$

Figure 10 Contour stream lines for different values x_d , $\phi=0.2$ and $\beta=0.1$, $\theta_0=00.4$ for $\delta=0.05$, $C=0.1$

$\phi=0.02$



$\phi=0.3$

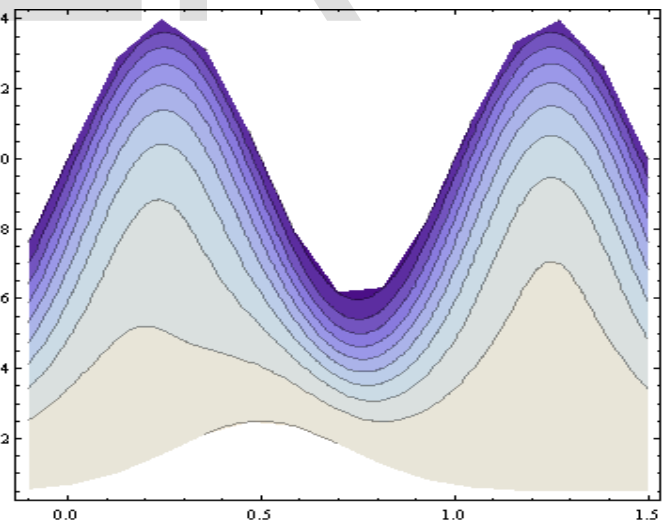


Figure 11 Contour stream lines for different values ϕ , $\delta=0.2$ and $\beta=0.1$, $\theta_0=00.4$ for $z_d=0.0$, $C=0.1$

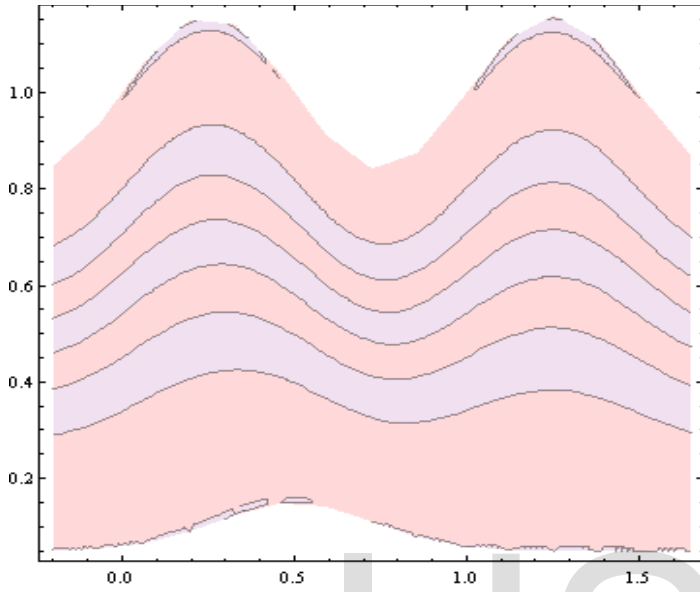


Figure 12 Contour stream lines for $\theta_0=7.4$,
 $\varphi, \delta=0.2$, $\beta=0.1$, $z_d=0.0$, $C=0.1$

IJSER